Journal of Applied Polymer Science

Polypropylene/Polyethylene Blends as Models for High-Impact Propylene-Ethylene Copolymers, Part 2: Relation Between Composition and Mechanical Performance

Cornelia Kock,[1] Nicolai Aust,[2] Christelle Grein,[1,3] Markus Gahleitner[1]

[1]Borealis Polyolefine GmbH, Innovation Headquarters, St. Peterstraße 25, Linz 4021, Austria

[2]University of Leoben, Chair of Chemistry of Polymeric Materials, Otto-Glöckel-Strasse 2, Leoben 8700, Austria

[3]SABIC Europe, 6130 PD Sittard, The Netherlands

Correspondence to: C. Kock (E-mail: cornelia.kock@borealisgroup.com)

ABSTRACT: The relation between composition and mechanical performance of a series of binary polyolefin blends was studied in this article. A fractionation of these model compounds with temperature rising elution fractionation (TREF) was applied to study the possibility to fractionate industrially relevant heterophasic polyolefin systems. The separation quality according to molecular structures or chemical composition was found to be good for most of the systems, but especially the separation of ethylene-propylene random copolymer and high density polyethylene by TREF turned out to be difficult if not impossible. An extensive mechanical characterisation including the determination of brittle-to-ductile transition curves showed significant effects of modifier type and amount. Toughness effects can be related primarily to the modulus differences between modifier and matrix. Compatibility and particle size only have a secondary influence, but must be considered for a detailed interpretation of the mechanics of the investigated systems. © 2013 Wiley Periodicals, Inc. J. Appl. Polym. Sci. 000: 000–000, 2013

KEYWORDS: polyolefins; blends; mechanical properties; copolymers

Received 9 January 2013; accepted 5 February 2013; published online
DOI: 10.1002/app.39181

INTRODUCTION

One of the major challenges in developing advanced PP copolymers, especially high-impact copolymers with ethylene as comonomer,[1–8] is to relate the molecular composition and the resulting phase structure to the final applicability. This application behavior is always expressed as a balance between processability, mechanical, and optical properties. This task can be broken down in practice into two major questions:

- How changes in catalyst system, polymerization conditions and comonomer feed[9–11] define the molecular composition (chain structure) and eventually the phase morphology.
- How these composition factors affect flow and solidification behavior, but also the balance between stiffness and toughness[2,4,5,12,13] and the optical performance.[14]

In the first part of this study[15] we focussed on the development of phase morphology as defined by component compatibility and rheology. A set of model blends based on different PP and PE types has been used for this purpose, which is further investigated in the present article. It was concluded that at rather constant viscosity ratio between matrix PP phase and disperse PE phase as well as composition, respectively, chain structure changes on both sides can change the particle size distribution significantly through a change in interfacial tension.

To study composition effects of multimodal polymers on the final property profile, model compounds are the systems of choice, since all components of the final material can be analyzed separately as well. By fractionating the model compounds, the possibility and quality of fractionating polyolefin blends can be evaluated. The knowledge gained this way can then be applied to industrially relevant heterophasic systems, which are generally produced in multistage reactor systems.[9]

Temperature rising elution fractionation (TREF) is the most widely used technique to fractionate semicrystalline polymers according to their solubility-temperature behavior and therefore by their molecular structures or chemical composition distributions.[16–23] TREF can be divided into two main steps, namely the crystallization and the elution step. Before the first step the polymer is dissolved at elevated temperatures in a good solvent. Then it is precipitated, respectively, crystallized under well controlled conditions by slowly decreasing the temperature. In the second step, the polymer is eluted in reverse order to the one it

was precipitated. TREF can be operated analytically[17,19,22,23] and preparatively.[16,20] In analytical TREF (aTREF), the eluted polymer is continuously monitored by an online detector [mass or concentration detector, e.g., a refractive index (RI) detector]. Preparative TREF (pTREF) is a separation technique in which polymer fractions are taken at predetermined temperature intervals and subsequently characterized to determine their microstructure offline. A key question for both operation modes is the resolution, that is, the separation quality for chemically different components of the polymer.

Both techniques have been applied in this study as complements to the rheological and electron-microscopic techniques presented before[15] to assess the microstructure of the model blends. They will allow a deeper level of understanding when correlated to the molecular composition on the one and to the mechanical performance on the other hand.

EXPERIMENTAL WORK

A model blend series based on two different base (matrix) polymers, a PP homopolymer and a homogeneous ethylene-propylene (EP) random copolymer and three different PE modifier types (HDPE, LLDPE, and an ethylene-*co*-octene plastomer, EOC[20,21]) was investigated. The components were selected such that the viscosity ratio between matrix and disperse phase remained approximately constant; details of selection, composition, and blend preparation can be found in our previous article.[15] Also the determination of the particle size distributions based on transmission electron microscopy has been described there.

For the TREF analysis, the key process is the sample crystallization. Secondary effects like co-crystallization or molar mass influences during crystallization should be avoided. Furthermore, no effect of the molar mass was found on the elution temperature when molar masses are higher than 10,000 g/mol.[16] Aust et al.[22] investigated the effect of different run parameters on the separation efficiency of TREF with the aid of a factorial design experiment. They found that an elevated starting temperature for crystallization along with low cooling and heating rates are beneficial for peak separation.

For PP homopolymers, TREF-eluograms represent the tacticity distribution due to the materials' stereo- and regio-regularity, which is affecting its crystallinity. Viville et al.[24] found that TREF is not only fractionating according to tacticity, but also according to the longest crystallizable sequence in a chain. In random copolymers, fractionation occurs according to comonomer (in our case, ethylene) content, which mainly affects the crystallinity here.[25] TREF of heterophasic polypropylene leads to a mixture of amorphous EP random copolymer (EPR), crystallizable EP copolymer (EPC), propylene homopolymer and a minor part of polyethylene homopolymer.[17,20–23] Copolymers of similar content of ethylene and propylene are essentially amorphous and thus eluted at room temperature (often called "cold fraction"). Copolymers of high ethylene-content are crystallizable[19,21,24] and elute at higher temperatures.

The analytical TREF (aTREF) was performed with the aTREF-equipment TREF 200+ from Polymer Char S.A., Valencia, Spain. 1,2,4-Trichlorobenzene stabilized with 0.02 wt % 2,6-di-*tert*-butyl-(4-methyl phenol) (BHT) was used as the solvent. Standard analyses were done with a crystallization and elution rate of 0.5°C min^{-1}. The elution temperatures to separate the samples by pTREF were obtained from these eluograms.

Table I. Temperature Profile of Analytical TREF

	Rate (°C min^{-1})	Temperature T (°C)	Time t (min)	Stirring (rpm)
Dissolution	40	160	60	Disc
Stabilization	40	95	30	200
Crystallization	0.2	-	-	-
Stabilization	-	40	45	-
Elution	1	140	-	-

pTREF was done with the pTREF-equipment PREP of Polymer Char S.A., Valencia, Spain. As solvent p-xylene stabilized with 0.07 vol % BHT was used. For standard-separation, the crystallization rate was set to be 0.1°C min^{-1}. To obtain a better separation, the rate was changed to 0.25°C min^{-1} for PPHD20. The collected fractions were subsequently blended with the same amount of acetone and stored over night at 5°C allowing the polymer to precipitate completely. The precipitate was then filtered and dried in a vacuum oven at 54°C for 4 h to remove the remaining solvents. The quality of the fractionation was controlled by a subsequent aTREF-analysis. The exact temperature profiles used for fractionation are gathered in Tables I and II.

The single fractions of the pTREF were analyzed by differential scanning calorimetry (DSC) and size exclusion chromatography (SEC). In both cases, the same procedures as in our earlier article[15] were applied. In DSC, melting and crystallization behavior of the compositions were determined according to ISO 11357 with a TA-Instruments (Germany) 2920 Dual-Cell instrument using a heating and cooling rate of 10°C min^{-1} in a heat/cool/heat cycle between 23 and 210°C. In SEC, the MWDs of the samples were determined at 135°C with a GPC 220 chromatograph (Polymer Laboratories, Church Stretton, UK) equipped with a differential RI (DRI) detector (Polymer Laboratories) and a differential viscometer 210 R (Viscotek, Houston, TX).

For an overall thermo-mechanical profile, dynamic mechanical analysis (DMA) was performed in accordance with ISO 6721 with 50 × 10 × 1 mm^3 compression molded samples, as a function of temperature at a test frequency of 1 Hz with a

Table II. Temperature Profile of preparative TREF

	Rate (°C min^{-1})	Temperature T (°C)	Time t (min)	Stirring (rpm)
Dissolution	20	130	60	200
Stabilization	20	95	45	150
Crystallization	0.1[a]	20	20	0
Fractionation	20	Individually set	60	150

heating rate of 2 K min^{-1}. Measurements were carried out under forced oscillation in a torsion mode ($\varepsilon = 0.04\%$) with an ARES rheometer (Rheometric Scientific, Piscataway, NJ). Temperature dependence of storage modulus G' and loss angle tangent tan(δ) were used for evaluation as outlined earlier.[26]

DMA is a helpful tool to correlate thermo-mechanical properties to mechanical ones since a simple relationship between torsional and elastic modulus exist.[27] Furthermore, the increasing mobility of the material with increasing temperature can be related to the impact strength. In two earlier articles,[26,28] we found that the molecular relaxations measured by DMTA and Charpy impact testing correlate quantitatively if all samples show unstable crack propagation. If changes in the failure mode occur, qualitative correlations remain. The area under the relaxation peaks represents the relaxation strength and is hence a direct indicator of the damping behavior of the material.[26,29] The area below the β-relaxation peak of iPP named ATD(PP) is a measure of the molecular mobility of the matrix. The area under the α-transition peak of the EPR ATD(EPR) of heterophasic copolymers accounts for the mobility of the elastomer particles.

The final stiffness and toughness profile of the blends was determined mostly with standardized mechanical tests on injection-molded specimens of 80 × 10 × 4 mm prepared in accordance with EN ISO 1873-2 after a conditioning time of 96 h. Flexural tests in accordance with ISO 178 were performed on a Zwick Universaltester (Zwick/Roell, Ulm, Germany) with a robotic auto sampler. The test was conducted with a preload of 1*N* and a velocity of 2 mm min^{-1}. The E-modulus was determined in the range of 0.05–0.25% strain of the outer fiber. Standard impact strength of the materials was determined using notched Charpy impact tests at 3.8 m s^{-1} according to ISO 179-2/1eA at +23 and −20°C.

The determination of the brittle-to-ductile transition temperature (BDTT) was done to gain deeper insight into the fracture behavior.[5,30,31] The necessary measurements were carried out on an instrumented Charpy device (Roell Amsler RKP50 (Zwick/Roell, Ulm, Germany) with a 50J pendulum and a test speed of 1.5 m s^{-1} using single etched notched bending specimens (a/W = 0.25) following ISO179 (geometry as in 1eA). The interpretation of the results was done in several ways. A sharp incurvature in the plot of the total fracture energy G_{tot} over the temperature can be associated with the brittle-to-ductile transition. Another possibility is the interpretation of the fracture areas of the specimens after the test, with the first occurrence of stress-whitening indicating semiductile fracture. Furthermore, the force-displacement curves taken at each temperature can be used to determine the brittle-to-ductile transition since ductile behavior shows a different characteristic in these diagrams.

RESULTS AND DISCUSSION

Analytical TREF

The fractionation analysis was started with the pure blend components, for which the aTREF eluograms are summarized in Figure 1. Studying the base polymers an increase in peak elution temperature from the random copolymer to the PP-homopolymer is found, indicating an increase in matrix crystallinity. The

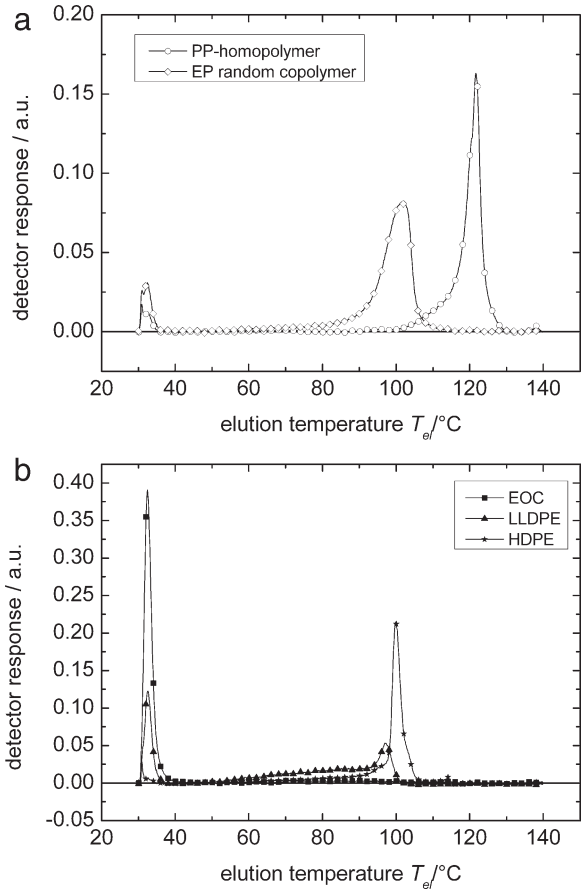

Figure 1. aTREF-eluograms of (a) the base polymers and (b) the modifier polymers.

reduced crystallinity of the random copolymer is caused by the random incorporation of ethylene units in the PP chain, which inhibits the crystallization by disrupting the 3_1-helix of PP, while the amorphous part (cold elution peak) is clearly increased. The eluograms of the modifier polymers reflect very well their differences in structure and crystallinity: While the plastomer is eluting completely at room temperature, the HDPE shows a sharp peak at 100°C reflecting its high crystallinity and narrow composition distribution. The LLDPE is eluting over the whole temperature range from room temperature to 100°C. This behavior is due to copolymerization with butene in production and the resulting short chain branching distribution (SCBD) in the polymer.

All model compounds based on the PP homopolymer show distinct peaks of the base polymer, modifier polymer, and amorphous fraction allowing for preparative fractionation (see Figure 2). By separating and characterizing the amorphous and crystalline copolymers originating from the base polymer as well as from the modifier, it is expected to gain deeper insight in the relation between molecular composition and end-use properties. However, due to the low crystallinity of the EP random copolymer the peaks of this base polymer overlap totally with those of the polyethylenes. Consequently, these model compounds cannot be separated by pTREF. By applying crystallization analysis

Applied Polymer SCIENCE

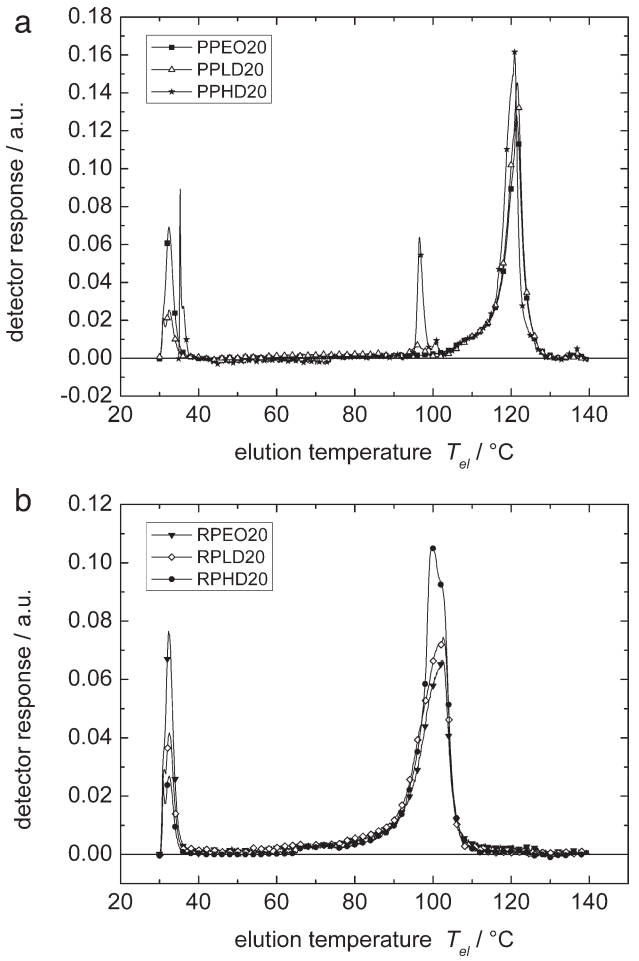

Figure 2. Differential aTREF eluograms of model compounds with different modifier polymers based on (a) PP homopolymer and (b) EP random copolymer.

fractionation (CRYSTAF)[32] with optimized run parameters a profile of high quality showing separated peaks for the components could be achieved.[33]

pTREF with Follow-Up Analysis

The three model compounds based on the PP homopolymer and the one based on the EP random copolymer with the EOC as modifier were fractionated preparatively. Table III lists the cutting temperatures and the weight fraction distribution for all investigated compositions. The separation quality was subsequently controlled by aTREF of the fractions. The noncrystalline part originating from the base polymer as well as from the modifier was collected as well as the crystalline matrix and the (semi)crystalline part of the modifier. Since the experimentally determined amount of fractions is in good accordance with the one determined by integration of the respective peaks in the aTREF-eluograms the quality of separation was high.

Figure 3 shows the aTREF-eluograms of the fractions of PPLD20 and PPHD20. Since pTREF is separating PE according to its SCBD the LLDPE of PPLD20 was also fractionated according to this characteristic. The third fraction of PPLD20 is representing the LLDPE with narrow short-chain branching distribution (SCBD) crystallizing at higher temperatures. The second fraction is eluting from 40 to 90°C because of its short chain branching and resulting broad crystallization range. Figure 3(b) shows the four fractions of PPHD20. Due to the high crystallinity of HDPE its elution range overlaps partially with the one of the base polymer. Thus an intermediate fraction containing PP and HD was collected, since a total separation of these two polymers was not possible. From a comparison of the two graphs, one can easily see the differences in crystallization behavior of LLDPE and HDPE. Latter is hardly having a noncrystallizable amount and the narrow shape of the elution peak is pointing out its narrow crystallization range.

DSC was used to determine the composition of the fractions, since melting and crystallization temperatures of the composing polymers are known. However, multiple peaks in the DSC-thermograms can occur since the aTREF-profiles sometimes show broad distributions and overlaps, indicating the complexity of the fractions. Zacur et al.[19] reported that due to the tacticity distribution of PP the elution ranges of PP and the crystalline copolymers overlap. A total separation of these components will be challenging. Nevertheless, DSC is a powerful tool to distinguish between amorphous EPR, semicrystalline EPC, and crystalline PE and PP.

The DSC traces of the first fractions of the blends showed broad peaks with several shoulders indicating a build-up by noncrystallizable material of base and modifier polymer. For the HDPE modified sample, already the second fraction contains some PP next to crystalline PE (see Figure 4). Martuscelli et al.[34] investigated the crystallization behavior of HDPE/PP from the melt, reporting that the presence of HDPE hinders the crystallization of PP (a fact, which was confirmed for the systems under

Table III. Characteristics of pTREF: Cutting Temperatures, Rate of Yield, and Weight Percentage of Each Fraction (Normalized to 100% Rate of Yield)

Sample code	Number of fractions	Cutting temperatures $T_{cutting}$ (°C)	Rate of yield (%)	Weight percentage of fractions (wt %)
PPEO20	2	40/120	99.6	22.0/78.0
PPLD20	4	35/80/91/120	88.2	6.4/12.2/8.0/73.4
PPHD20	4	35/92/100/120	85.7	2.6/15.3/11.6/70.5
RPEO20	2	40/120	99.5	26.7/73.3

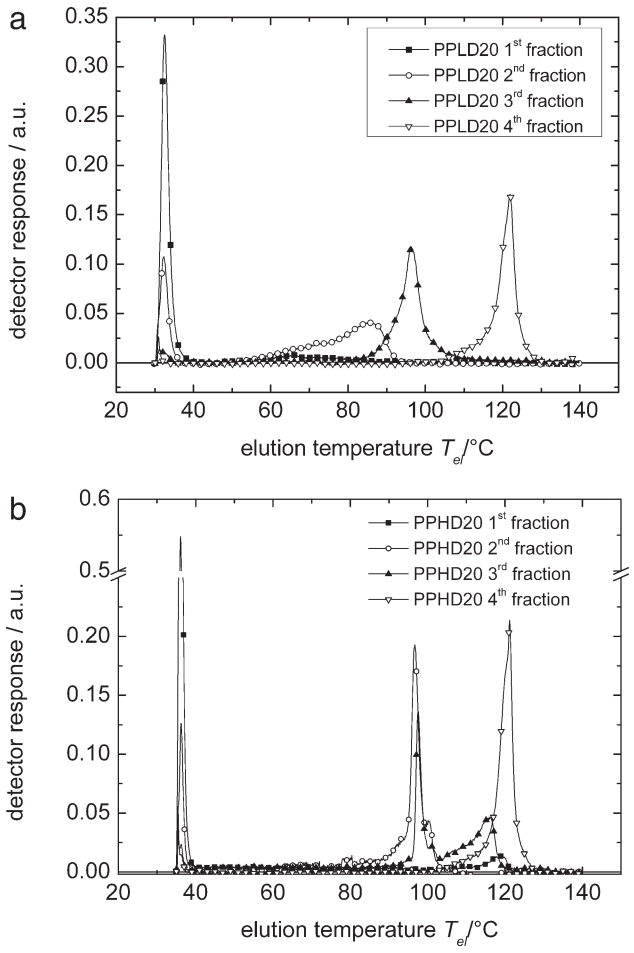

Figure 3. aTREF eluograms of pTREF fractions from (a) the PPLD20 blend and (b) the PPHD20 blend.

investigation in our earlier article; see Table II of Ref. [15]). This may explain why PP-melting points were found in all fractions of PPHD20. The presence of the HDPE in the blend inhibits the crystallization of PP-fractions, which leads to the elution in lower crystalline fractions of pTREF. While the situation in melt[34] and in solution (TREF) cannot be compared directly, it must be considered that the concentration in pTREF is relatively high (6 mg mL^{-1}) and the solutions are stirred during the crystallization process. The mechanical field introduced during the stirring process enables the macromolecules to be stretched and partially orientated. This leads to a change in the end-to-end-distance of the molecule and hence to a change of the thermodynamic interaction parameter.[35] Consequently, the mechanical field will also influence the binodals and spinodals of the phase diagram. It is suggested that the stirring led to changes in the interaction parameter, which impeded the transfer of the results achieved by aTREF to pTREF.

For the LLDPE modified sample, the separation of PE and PP was possible in a higher quality. The second fraction consists of PE having a broad SCBD leading to reduced crystallizability and a broadening in melting and crystallization peaks. The melting curve of the third fraction showed the expected sharp melting peak for highly crystalline PE. The fraction eluting in the high temperature range was composed exclusively of isotactic PP homopolymer (see Table IV).

SEC was done for all the blend fractions. The first fractions containing the noncrystallizable part of the materials shows a relatively low molecular weight originating most probably from short chains of noncrystallizable matrix material (PP). A comparison of the molecular weight distribution of the single fractions with those from the components of the fractions showed a good alignment of the curves indicating a high quality of separation.

Figure 5 shows the MMDs of the fractions of PPLD20. As Figure 5(a) shows, the modifier polymer itself was separated into two fractions of different SCBD. This fractionation combined with subsequent SEC analysis shows that the fraction eluting at higher temperature (narrow SCBD) has a lower molar mass than the fraction with a broad SCBD. This molecular composition is a consequence of the bimodal production process. The low molar mass polyethylene (resembling HDPE) is produced without any comonomer-feed in the loop reactor, while in the second reactor polyethylene of higher molar mass is produced in the presence of a comonomer (here butene). This production method leads to a bimodal molar mass distribution of the polyethylene fraction having short chain branching and a more monomodal distribution for the non-branched PE. Figure 5(b) presents an overview of all fractions recovered from the compound, showing the dominant matrix polymer curve (fourth fraction) and a calculated summary curve.

DMA Investigations

The DMA traces of the model compounds based on PP are shown in Figure 6 and their shape follows expectations. For the PPHD20 and PPLD20 only the typical PE-transition at −120°C is found, while the PPEO20 shows a strong damping peak at −60°C.

It can be stated that no pronounced shifts in transition temperatures of the components took place considering the curves of the model compounds. This indicates immiscibility of the materials in the solid state. Comparing the effects of different modifiers on the relaxation behavior of the blends leads to the conclusion that the mobility of the matrix is least affected by the addition of the plastomer. The addition of polyethylene however, leads to reduced relaxation strengths of the β-transition of the matrix. This is also reflected by the reduced values of the area under the tanδ peak of the β-transition of PP [ATD(iPP)] of blends modified with PE compared with that containing the plastomer (see Figure 6). The addition of plastomer might lead to a change in the relaxation strength of the matrix, caused by an enhanced mobility of the chains.

The storage modulus G' measured at 23°C indicates the stiffness of the materials, with lowest values for the plastomer modified blends whereas the highest moduli were found for the HDPE modified compounds. This was expected since the plastomer was the softest modifier polymer and HDPE the stiffest. Table V is gathering all results from DMA.

Applied Polymer SCIENCE

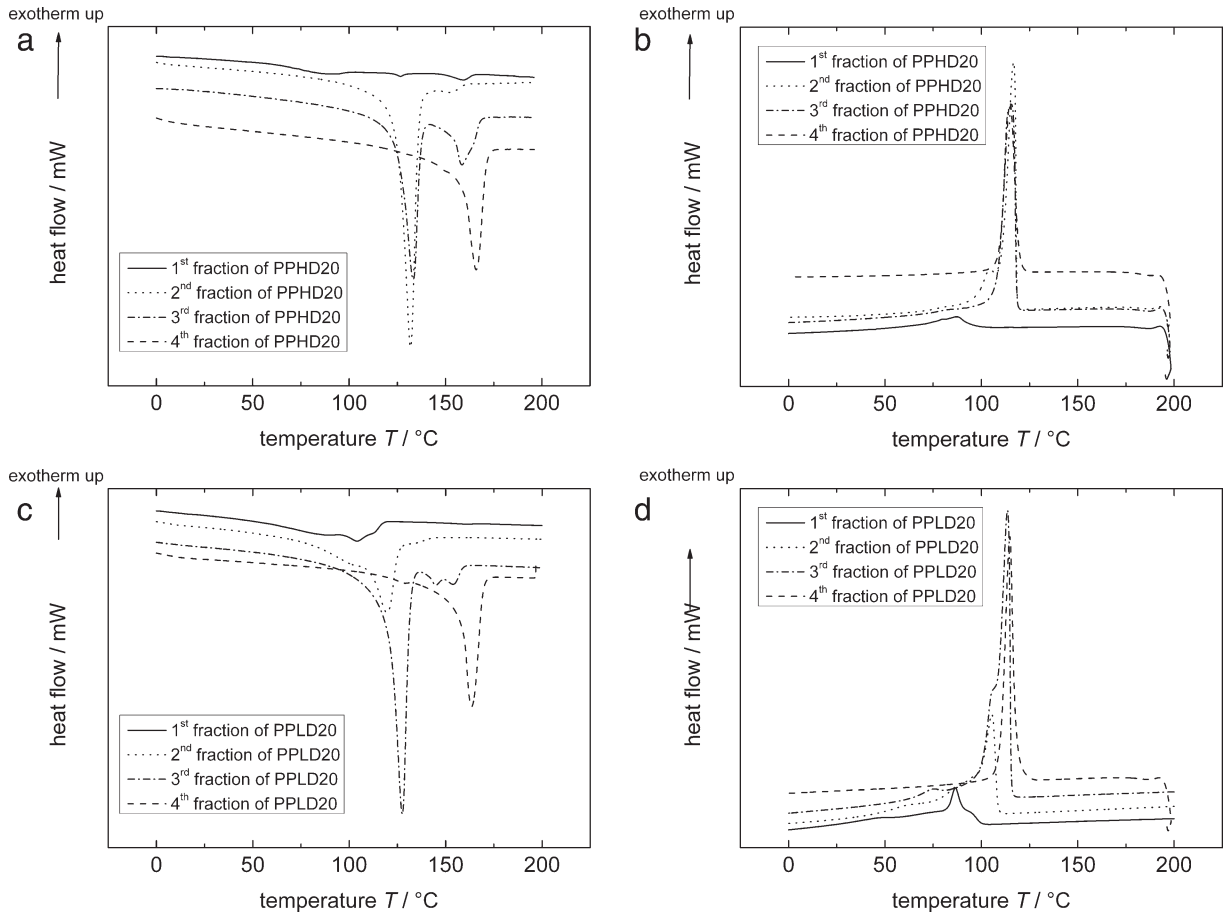

Figure 4. DSC-traces of PPHD20 (a) melting endotherms and (b) crystallization exotherms and DSC-traces of PPLD20 (c) melting endotherms and (d) crystallization exotherms; for the sake of clarity the baselines of the curves are shifted along the y-axes.

Mechanical Performance

Materials showing high stiffness combined with good impact behavior are desirable in most application areas, but very challenging to develop. Table V summarizes characteristic values for stiffness as well as impact behavior.

Moduli as key indicator of the material stiffness are a measure to quantify the resistance of the specimen to mechanical deformation. At a constant loading of rubber, the main influencing factor on the modulus is the crystallinity of the matrix.[36,37] Increasing amount of rubber decreases the volume of the stiff matrix and thus the modulus.[38] The effect of the addition of different modifiers to the base polymers was comparable for all compounds. The softness of the plastomer leads to a remarkable reduction of the flexural modulus as expected, whereas the addition of highly crystalline HDPE results in stiffness comparable to that of the base material. A relatively good correlation between the G' (23°C) and the flexural modulus is shown in Figure 7, despite the differences specimen geometry and processing.

Not just modulus effects, but also toughness effects can be related primarily to the modulus differences between modifier and matrix. In contrast to other studies, where merely concentration effects have been studied,[4,38–41] the variation in deformability of the modifier particles between HDPE and the C2C8-

Table IV. Analytical Results from pTREF Fractions of the Blend PPLD20

	DSC				GPC	
Fraction (temperature range)	T_m (PE; °C)	H_m (PE; J/g)	T_m (PP; °C)	H_m (PP; J/g)	M_w (kg/mol)	M_w/M_n
1 (<35°C)	89	42	-	-	221	18.4
2 (35-80°C)	120	114	-	-	197	9.4
3 (80-91°C)	128	142	154	18	174	5.1
4 (91-120°C)	-	-	163	118	357	3.1

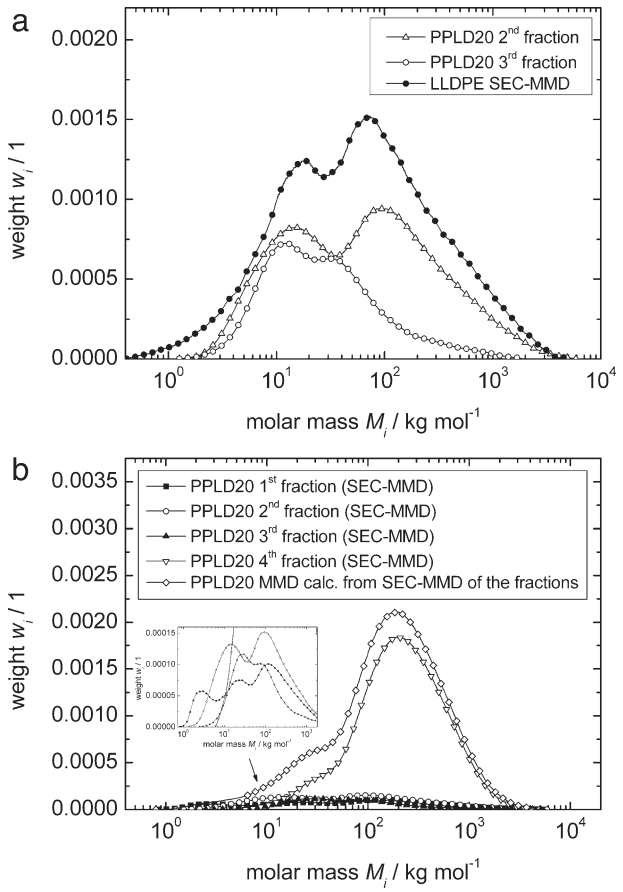

Figure 5. MMDs of fractions of PPLD20 (a) second and third fraction building up the LLDPE compared with pure LLDPE and (b) all fractions of PPLD20 and the corresponding calculated MMD of the compound.

plastomer is significant in this case and clearly reflected in fracture resistance. Normally the toughness, that is, the resistance to dynamic loading, of blends is considered primarily to be a function of morphological parameters like volume fraction and particle size of the dispersed phase. In this case, the relatively smallest particles achieved for LLDPE[15] are clearly overruled in terms of toughness by the lower modulus of the plastomer. The ability of inclusions to enhance the toughness of a polymer is directly related to its stress-concentration ability, being a direct function of the modulus differences between dispersed phase and matrix.[42] This effect of modulus difference—highest for PPEO20, lowest for RPHD20—is clearly reflected in the relative toughening effect at room temperature.

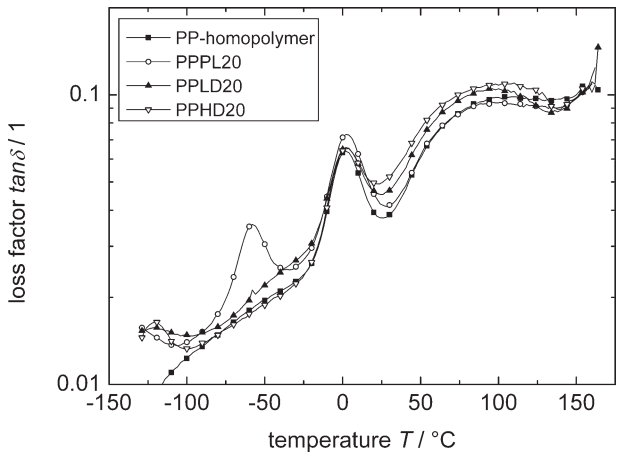

Figure 6. DMA traces of the model compounds based on the PP-homopolymer.

The biggest toughening effect is achieved for RPEO20, despite the smaller modulus difference as in case of PPEO20. This is due to smaller particles with more uniform particle size distribution compared to compounds based on the homopolymer. A higher degree of compatibility will consequently enhance toughness via the morphology.[6,39,43,44] Additionally, phase adhesion and even cocrystallization at the interface may contribute to the higher impact strength.

With the PP/PE combinations investigated here, no significant impact enhancement at low temperatures was achieved. As can be seen from the DMA-traces (Figure 6), the modifier particles are at least partly already in their glassy state when tested under dynamic conditions. The particles are thus unable to create a great extent of crazing at any stage of crack formation.[38,45] Consequently, crazing is insufficient and becomes overtaken by fast propagating cracks resulting in low impact and brittle failure.

The resistance of the material against unstable crack propagation can be described by the brittle-to-ductile transition, which is defined as a significant increase in the impact strength at a certain temperature or test speed. It is connected to a change in the deformation mechanism from predominantly crazing to predominantly shear yielding. By increasing the temperature the yield stress decreases, whereas the fracture stress remains more or less unaffected. The yield stress drops below the fracture stress at the brittle-to-ductile transition. The BDTT can be used to describe the effectiveness of toughening and application range of a material.[4,5,26]

A plot of the total dissipated energy G_{tot} versus temperature for model compounds based on the PP homopolymer with different amounts of polyethylene is shown in Figure 8. The BDTTs were determined as the inflection point of these curves. The influence of different concentrations of modifier can be seen easily. Both HDPE and LLDPE modifications have a positive influence on the toughness as highlighted by the fact that with increasing amount of modifier the BDTT is shifted to lower values. Starting at ~+70°C, especially the addition of LLDPE shifts the transition to ~45°C as seen in Figure 9. The higher amount of modifier increases the extent of stress concentration and reduces the yield stress of the material. An enhanced toughening effect occurs as consequence of a higher amount of dispersed phase.[37]

Remarkably although, the BDTT is largely independent of the HDPE concentration in the thus modified compositions, staying at ~ +50°C for all levels. The fact that the modulus difference between matrix and modifier is much more limited in this case obviously causes the particles to lose their ability to act as stress concentrators.[46] As a result, only a very limited impact modification can be observed for these compounds (see also Table V).

Table V. Overview of Blend Composition and Mechanical Performance from DMA and Standard Tests (NIS: Notched Impact Strength)

Sample code	ATD (β)	Storage modulus G' (23°C; MPa)	Flexural Modulus (MPa)	Charpy NIS (23°C; kJ m^{-2})	Charpy NIS (−20°C; kJ m^{-2})
PP	0.68	840	1620	3.5	1.6
EP RACO	1.47	430	790	9	1.8
PPEO20	0.87	525	1050	21	2.1
PPLD20	0.61	670	1255	8	1.5
PPHD20	0.53	740	1530	6	1.5
RPEO20	1.65	280	535	70	2.1
RPLD20	1.16	425	720	17	1.2
RPHD20	0.91	500	925	13	1.5

The effect of particle size on the brittle-to-ductile transitions is, according to the literature, clearly complex. Jang et al.[46] reported that smaller particles could initiate yielding which leads to tough behavior and reduced transition temperatures. It seems that the influence of the particle size is dependent on the dominant deformation mechanism, and that bigger particles may be advantageous in case of crazing as dominant mechanism, whereas small particles are beneficial if yielding takes place. Van der Wal[37] reports that bigger particles are more influential on the impact behavior since they may form larger cavities, which are more likely to become unstable.

Conclusions in this respect are difficult from this study, as the viscosity ratio was selected in a way to have the relative phase compatibility as main defining factor for the particle size.[15] This compatibility is, however, necessarily connected to the aforementioned modulus difference and thus dependent factor.

CONCLUSIONS

In a continuation of our previous study of rheology-morphology interactions,[15] the relation between composition and mechanical performance of a series of binary polyolefin blends was studied. A fractionation of the model compounds with TREF was applied to study the possibility to fractionate industrially relevant heterophasic polyolefin systems. The separation quality according to molecular structures or chemical composition was found to be good for most of the systems, but especially the

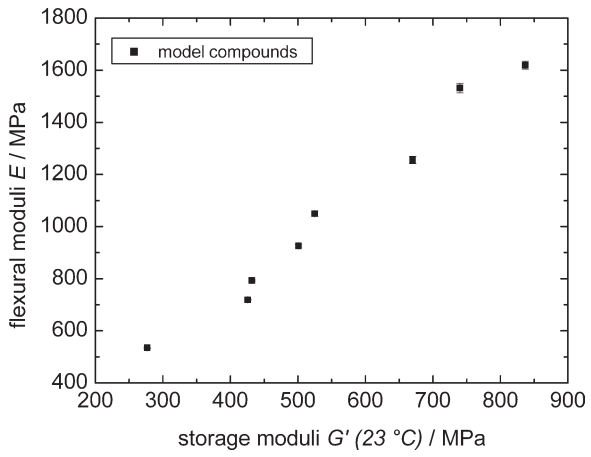

Figure 7. Correlation between flexural moduli (ISO 178) and the storage moduli G' (23°C) from DMA.

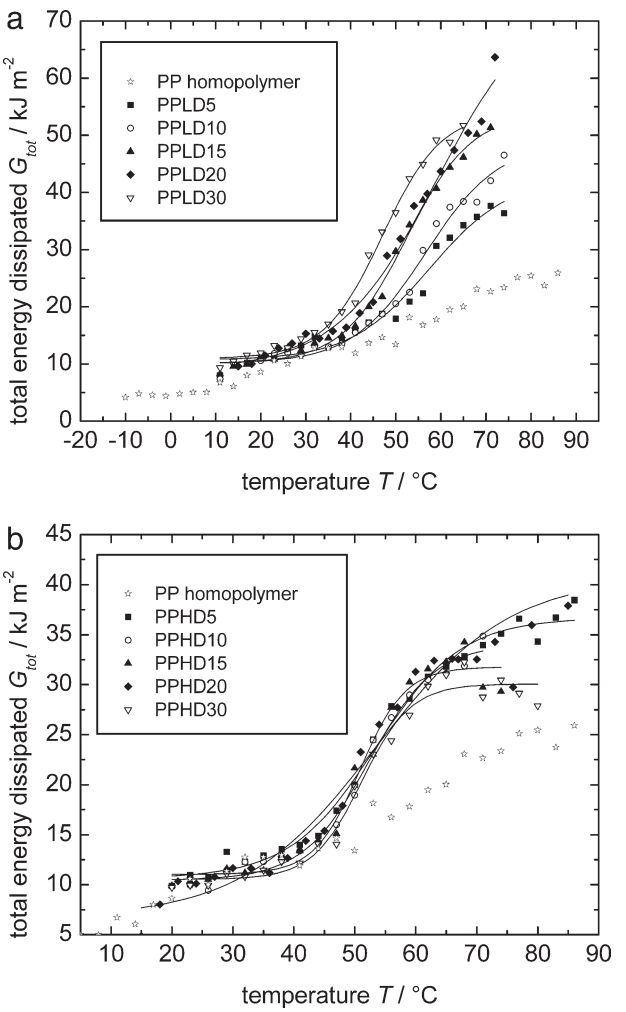

Figure 8. Total energy dissipated (G_{tot}) plotted against temperature for model compounds based on the PP homopolymer (a) modified with different amounts of LLDPE and (b) modified with different amounts of HDPE.

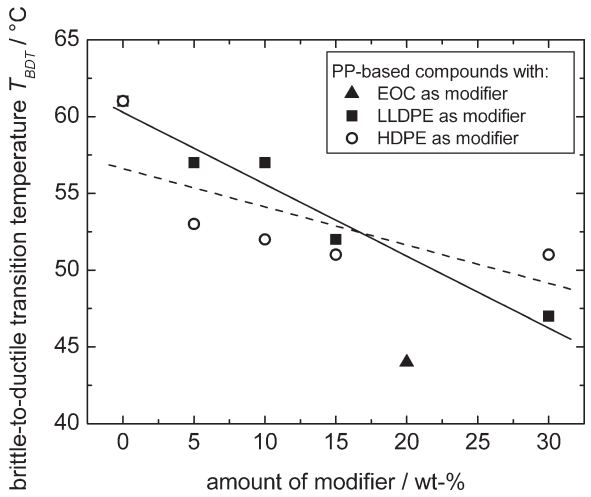

Figure 9. BDTT as a function of modifier content for PP homopolymer based blends with HDPE, LLDPE, and EOC.

separation of EP random copolymer (EP-RACO) and high density polyethylene (HDPE) by TREF turned out to be difficult if not impossible. Alternative approaches like the CRYSTAF technique give a clear advantage here.

An extensive mechanical characterisation including the determination of brittle-to-ductile transition curves showed significant effects of modifier type and amount. The modulus can be explained by a simple mixing rule, and the relative difference in modulus between modifier and matrix is clearly the main defining factor for toughness as well. The largest modulus difference appears in the plastomer modified model compounds, while the lowest appears in the HDPE modified compounds. This is clearly reflected both in the relative toughening effect at room temperature. Compatibility and particle size only have a secondary influence, but must be considered for a detailed interpretation of the mechanics of the investigated systems. As in this study, the viscosity ratio was selected such that the relative phase compatibility is the main defining factor for the particle size; this compatibility is necessarily connected to the modulus difference, making it a dependent factor.

ACKNOWLEDGMENT

Parts of the research work of this paper was performed at the Polymer Competence Center Leoben GmbH (PCCL, Austria) within the framework of the COMET-program of the Federal Ministry for Transport, Innovation and Technology and Federal Ministry for Economy, Family and Youth with contributions by the Johannes Kepler Universität Linz, the University of Leoben and the Borealis Polyolefine GmbH Linz. The PCCL is funded by the Austrian Government and the State Governments of Styria and Upper Austria.

REFERENCES

1. Ramsteiner, F., Kanig, G., Heckmann, W., Gruber W. *Polymer* **1983**, *24*, 365.
2. Hayashi, K., Morioka, T., Toki, S. *J. Appl. Polym. Sci.* **1993**, *48*, 411.
3. Starke, J. U., Michler, G. H., Grellmann, W., Seidler, S., Gahleitner, M., Fiebig, J., Nezbedova, E. *Polymer* **1998**, *39*, 75.
4. Grellmann, W., Seidler, S., Jung, K., Kotter, I. *J. Appl. Polym. Sci.* **2001**, *79*, 2317.
5. Grein, C., Bernreitner, K., Hauer, A., Gahleitner, M., Neißl, W. *J. Appl. Polym. Sci.* **2003**, *87*, 1702.
6. Grein, C., Gahleitner, M., Knogler, B., Nestelberger, S. *Rheol. Acta* **2007**, *46*, 1083.
7. Li, Y., Xu, J.-T., Dong, Q., Fu, Z.-S., Fan, Z.-Q. *Polymer* **2009**, *50*, 5134.
8. Zhang, C., Shangguan, Y., Chen, R., Wu, Y., Chen, F., Zheng, Q., Hu, G. *Polymer* **2010**, *51*, 4969.
9. Cecchin, G., Morini, G., Pelliconi, A. *Macromol. Symp.* **2001**, *173*, 195.
10. Kittilsen, P., McKenna, T. F. *J. Appl. Polym. Sci.* **2001**, *82*, 1047.
11. Bouzid, D., McKenna, T. F. L. *Macromol. Chem. Phys.* **2006**, *207*, 13.
12. Kim, G. M., Michler, G. H., Gahleitner, M., Fiebig, J. *J. Appl. Polym. Sci.* **1996**, *60*, 1391.
13. Grein, C., Kausch, H.-H., Béguelin, Ph. *Polym. Test.* **2003**, *22*, 733.
14. Cecchin, G. *Macromol. Symp.* **1994**, *78*, 213.
15. Kock, C., Gahleitner, M., Schausberger, A., Ingolic, E. *J. Appl. Polym. Sci.*, to appear. DOI: 10.1002/APP.38289.
16. Wild L. *Adv. Polym. Sci.* **1991**, *98*, 1.
17. Usami, T., Gotoh, Y., Umemoto, H., Takayama, S. *J. Appl. Polym. Sci.: Appl. Polym. Symp.* **1993**, *52*, 145.
18. Soares, J. B. P., Hamielec, A. E. *Polymer* **1995**, *36*, 1639.
19. Zacur, R., Goizueta, G., Capiati, N. *Polym. Eng. Sci.* **1999**, *39*, 921.
20. Xu, J., Feng, L. *Eur. Polym. J.* **2000**, *36*, 867.
21. Pires, M., Mauler, R. S., Liberman, S. A. *J. Appl. Polym. Sci.* **2004**, *92*, 2155.
22. Aust, N., Gahleitner, M., Reichelt, K., Raninger, B. *Polym. Test.* **2006**, *25*, 896.
23. Mncwabe, S., Luruli, N., Marantos, E., Nhlapo, P., Botha, L. *Macromol. Symp.* **2012**, *313–314*, 33.
24. Viville, P., Daoust, D., Jonas, A. M., Nysten, B., Legras, R., Dupire, M., Michel, J., Debras, G. *Polymer* **2001**, *42*, 1953.
25. Gahleitner, M., Jääskeläinen, P., Ratajski, E., Paulik, C., Reussner, J., Wolfschwenger, J., Neißl, W. *J. Appl. Polym. Sci.* **2005**, *95*, 1073.
26. Grein, C., Bernreitner, K., Gahleitner, M. *J. Appl. Polym. Sci.* **2004**, *93*, 1854.
27. Fritzsche, C. *Kunstst. Plast.* **1974**, *21*, 17.
28. Gahleitner, M., Grein, C., Bernreitner, K., Knogler, B., Hebesberger, E. *J. Therm. Anal. Calorim.* **2009**, *98*, 623.
29. Jafari, S. H., Gupta, A. K. *J. Appl. Polym. Sci.* **2000**, *78*, 962.
30. Tan, H., Li, L., Chen, Z., Song, Y., Zheng, Q. *Polymer* **2005**, *46*, 3522.

31. Chen, Y., Chen, W., Yang, D. *J. Appl. Polym. Sci.* **2008**, *108*, 2379.
32. Kissin, Y. V., Fruitwala, H. A. *J. Appl. Polym. Sci.* **2007**, *106*, 3872.
33. Fischlschweiger, M., Aust, N., Oberaigner, E.R., Kock, C. *Macromol. Chem. Phys.* **2009**, *210*, 383.
34. Martuscelli, E., Pracella, M., Avella, M., Greco, R., Ragosta, G. *Macromol. Chem.* **1980**, *181*, 957.
35. Vshivkov, S. A. *Polym. Sci. Ser. A* **2009**, *51*, 858.
36. Van der Wal, A., Mulder, J. J., Oderkerk, J., Gaymans, R. J. *Polymer* **1998**, *39*, 6781.
37. Van der Wal, A., Nijhof, R., Gaymans, R. J. *Polymer* **1999**, *40*, 6031.
38. Tam, W. Y., Cheung, T., Li, R. K. Y. *Polym. Test.* **1996**, *15*, 363.
39. Lu, J., Wie, G. X., Sue, H. J., Chu, J. *J. Appl. Polym. Sci.* **2000**, *76*, 311.
40. Elmajdoubi, M., Vu-Khanh, T. *Theor. Appl. Fract. Mech.* **2003**, *39*, 117.
41. Pukanszky, B. *Polymer* **1995**, *36*, 1617.
42. Bucknall, C. B. Toughened Plastics; Applied Science Publications: London, **1977**, pp 359.
43. Liang, J. Z., Li, R. K. Y. *J. Appl. Polym. Sci.* **2000**, *77*, 409.
44. Doshev, P., Lach, R., Lohse, G., Heuvelsland, A., Grellmann, W., Radusch, H.-J. *Polymer* **2005**, *46*, 9411.
45. Karger-Kocsis, J. *Polym. Eng. Sci.* **1987**, *27*, 241.
46. Jang, B. Z., Uhlmann, D. R., Vandersande, J. B. *J. Appl. Polym. Sci.* **1985**, *30*, 2485.